

Gas-Phase Molecular Structures of Third Row Transition-Metal Hexafluorides WF₆, ReF₆, OsF₆, IrF₆, and PtF₆. An Electron-Diffraction and *ab Initio* Study

Alan D. Richardson,^{1a} Kenneth Hedberg,^{*,1a} and George M. Lucier^{1b}

Department of Chemistry, Oregon State University, Corvallis, Oregon 97331, and
Department of Chemistry, University of California, Berkeley, California 94720

Received January 5, 2000

The molecular structures of WF₆, ReF₆, OsF₆, IrF₆, and PtF₆ have been measured by electron diffraction from the gases, the last from both PtF₆ itself and from a vapor assumed to consist of a mixture of O₂ and PtF₆ obtained by heating the salt O₂PtF₆. For models of *O_h* symmetry the bond lengths in the first three members of the series are essentially identical, but the Ir–F and Pt–F bonds are respectively about 0.01 and 0.02 Å longer. Models of *D_{4h}* symmetry were also tested for ReF₆, OsF₆, and IrF₆ in which operation of the Jahn–Teller effect is thought possible. For these models the same trend was seen in the average bond-length values. The effect of three-atom multiple scattering was also investigated, and experimental estimates of the effects of vibrational averaging (“shrinkage”) on the distances were obtained. Normal-coordinate analyses based on the observed wavenumbers yielded stretching force constants consistent with the usual inverse bond-length/force-constant relationship. *Ab initio* molecular orbital optimizations of the molecules constrained to *O_h* symmetry were carried out at several levels of theory and basis-set size. Less extensive optimizations of ReF₆, OsF₆, and IrF₆ with *D_{4h}* symmetry were also carried out. The best overall agreement with both the experimental values and the distance trend for *O_h* symmetry was obtained with the Hay–Wadt (*n*+1)VDZ basis on the metals and the aug-cc-pVTZ on the fluorines at the MP2 level, but these bases with B3P86 and B3PW91 density functional theory were nearly as good and with B3LYP only slightly worse. The *D_{4h}* structures for ReF₆, OsF₆, and IrF₆ with the cited bases at the B3P86 level were slightly more stable (respectively 0.8, 2.6, and 1.4 kcal/mol) with the axial bonds shorter by about 0.04 Å in ReF₆ and 0.07 Å in OsF₆, but about 0.05 Å longer in IrF₆. The significance of these values is uncertain. The experimental bond lengths (*r_g*/Å) with estimated 2σ uncertainties for the models of *O_h* symmetry are W–F = 1.829(2), Re–F = 1.829(2), Os–F = 1.828(2), Ir–F = 1.839(2), and Pt–F = 1.852(2); the Pt–F value from the O₂PtF₆ sample was 1.851(2) Å. Although the experimental data neither confirm nor refute the existence of the Jahn–Teller effect in ReF₆, OsF₆, and IrF₆, they ensure that if present the distortion from *O_h* symmetry must be small.

Introduction

A large number of elements, both metals and nonmetals, form monomeric hexafluorides. The structures of nearly all the molecules have been studied in the gas phase by electron diffraction (GED) and found to be consistent with equilibrium octahedral symmetry. Among these molecules are four members of the sixth-period transition-metal series, WF₆,^{2,3} ReF₆,⁴ OsF₆,³ and IrF₆,³ which were found to have nearly identical bond lengths, a remarkable fact in view of the substantially different properties of the M⁶⁺ such as nuclear charge, magnetic susceptibility, and thermodynamic stability. The bond-length similarity in these four molecules has been verified by XAFS studies⁵ of the solids, but, surprisingly, the bond length in the fifth member of the series, PtF₆, was found to be about 0.02 Å longer. A more recent report of a neutron-diffraction investigation of powder samples of WF₆, OsF₆, and PtF₆ has appeared,⁶

Table 1. Previously Measured Bond Lengths in Third Row Transition-Metal Hexafluorides

	electron diffraction ^a			neutron diffraction ^{a,b}		XAFS ^c	
	<i>r_g</i> ^d /Å	<i>r_a</i> ^e /Å	ref	<i>r</i> /Å	ref	<i>r</i> /Å	ref
WF ₆	1.832(3)	1.831	2	1.825(5)	6	1.821(2)	5
	1.834 ^f	1.833(8)	3				
ReF ₆	1.832(4)	1.831	4			1.812(1)	5
OsF ₆	1.833 ^f	1.832(8)	3	1.831(9)	6	1.816(3)	5
IrF ₆	1.833 ^f	1.832(8)	3			1.822(2)	5
PtF ₆				1.850(4)	6	1.839(3)	5

^a The uncertainties from different investigations have slightly different meanings, but are essentially 2σ with account taken of possible systematic errors. Where uncertainties are not given, they are approximately those for the other distance type. ^b Averages of four values from *C_s* molecular symmetry in the crystal. ^c Uncertainties are average deviations. ^d Thermal average distance. ^e Distance most directly related to electron-diffraction intensities: *r_a* ≈ *r_g* – *l*²/*r*. ^f Calculated from the authors' data.

and here, too, the Pt–F bond was found to be longer than the others. The bond-length data from these studies are found in Table 1.

Since the physical properties of PtF₆ are consistent with the similarities and trends observed for this transition-metal group, the Pt–F bond length stands as an apparent anomaly. Because molecular structures in the gas and solid states occasionally

- (1) (a) Oregon State University. (b) University of California.
(2) Seip, H. M.; Seip, R. *Acta Chem. Scand.* **1968**, *20*, 2698.
(3) Kimura, M.; Schomaker, V.; Smith, D. W.; Weinstock, B. *J. Chem. Phys.* **1968**, *48*, 4001.
(4) Jacob, E. J.; Bartell, L. S. *J. Chem. Phys.* **1970**, *53*, 2731.
(5) Brisdon, A. K.; Holloway, J. H.; Hope, E. G.; Levason, W.; Ogden, J. S.; Saad, A. K. *J. Chem. Soc., Dalton Trans.* **1992**, 139.
(6) Marx, R.; Seppelt, K.; Ibbertson, R. M. *J. Chem. Phys.* **1996**, *104*, 7658.

differ, a check of the gas-phase structure of PtF_6 , which has heretofore not been measured, was certainly desirable. Accordingly, we undertook what promised to be a more or less routine GED study of its structure which ultimately led to this reinvestigation of the entire third row transition series of hexafluorides. The history of these reinvestigations began with the discovery that, just as it is in the solid, the M–F bond in gaseous PtF_6 is longer than in the other series members. For convenience these first experiments were done on the vapor of a volatilized sample of the salt O_2PtF_6 (PtF_6 is a powerful oxidizing agent capable of liberating F_2 from fluorides⁷ and of oxidizing O_2 to O_2^+ to yield O_2PtF_6 ⁸). The vapor from the salt was assumed to consist of an equimolar mixture of neutral O_2 and PtF_6 . However, there was a slight chance that the scattering molecules were not the supposed mixture of O_2 and PtF_6 but instead an adduct of the same composition as the crystalline sample: such an O_2PtF_6 “molecule” would be expected to have longer Pt–F bonds than in pure PtF_6 due to electrostatic repulsion. Several models of O_2PtF_6 adducts were found to give good fits to the diffraction data, but a disquieting feature to all was an oxygen–oxygen bond length almost identical to that in O_2 itself, whereas in the event of an adduct one expects some changes due to the interaction of the O_2 part with the PtF_6 . To settle the matter of the anomalous Pt–F bond length, the experiment was repeated with a sample of pure PtF_6 . The distance result was essentially identical to that obtained from the sample of O_2PtF_6 , thus making the hypothesized existence of an adduct in the vapors of this sample unlikely.

In order to be sure that the difference between the gas-phase structure of PtF_6 and the other members of the series was real, it was necessary to establish that there was no difference of scale between our experiment and the earlier ones from other laboratories on this transition-metal group of molecules. Such a difference can arise from small errors in electron accelerating voltages or camera distances. To help answer this question, the structure of IrF_6 , a sample of which was conveniently available, was reinvestigated. It was a surprise to find that the Ir–F bond, like the Pt–F one, was also longer than the average of the earlier gas-phase measurements of the W–F, Re–F, and Os–F distances, but the increase was only about half as much as the Pt–F. Although the evidence for significant differences of scale between ours and the earlier work was now weak, we decided to reinvestigate the structures of the remaining members of this transition-metal group to settle any remaining doubts. The hope was that experiments carried out under conditions as similar as possible would reveal any small differences between the gas-phase structures that might not presently be apparent. Among these conditions are questions of multiple (three-atom) scattering⁹ and vibrational averaging (“shrinkage”),¹⁰ each of which can affect the derived parameter values if appropriate corrections are not made. These questions had not been uniformly addressed in the earlier work.

The bond lengths for the other molecules found in these experiments were similar to those found by earlier investigators, and thus the possibility of a scale factor error as a cause of the larger Pt–F value is removed. The overall picture is now the following. The bonds in PtF_6 are clearly longer than in WF_6 , ReF_6 , and OsF_6 , which have nearly identical lengths. So is the bond in IrF_6 , but the increase is less than in the platinum compound. The bond lengths for the tungsten, rhenium, and

osmium compounds agree well with those from the earlier studies, taking into account the uncertainties in the measurements. This is also the case for the iridium compound, which has a rather large uncertainty from the earlier work. However, the overall notion, based on the earlier measurements of the first four members of the series in the gas phase, that the bond lengths are essentially constant throughout the entire series must be discarded in view of our more precise results for the iridium and platinum compounds.

Experimental Section

Samples of MF_6 (M = Re, Os, Ir, Pt) and O_2PtF_6 were prepared at the University of California at Berkeley, by G.M.L. and Professor Neil Bartlett. The commercial WF_6 sample was supplied by Professor Gary Gard of Portland State University. O_2PtF_6 was prepared as described by Edwards et al.,¹¹ but instead of being kept at 500 °C for several hours, the Monel reaction vessel was heated in a flame for about 15 min. Reactant quantities in millimoles were $\text{F}_2:\text{O}_2:\text{Pt} = 37:15:10.7$. OsF_6 and IrF_6 were prepared by heating the metals in Monel or stainless steel cans with an excess of fluorine at 250 °C for about 8 h. ReF_6 was also prepared in this fashion, but with the difference of a slight fluorine deficiency required to avoid ReF_7 production.

The instability of PtF_6 at elevated temperatures required use of an entirely different type of reactor for its preparation. For this reaction about 3 g of coiled Pt wire was hung from electrodes protruding from the top of a 0.5 L Monel can. Excess fluorine was condensed into the can at –196 °C. At this point its vapor pressure is about 300 Torr. With the can bottom immersed in a liquid N_2 bath, the wire was resistively heated. Once begun, the reaction became exothermic enough to be self-sustaining even if the wire broke to interrupt the electrical connection. As the PtF_6 is formed, it quickly condenses on the reactor walls, permitting yields as high as 70%.

The O_2PtF_6 samples were shipped to Oregon under an argon atmosphere in 20 cm Monel tubes sealed with Swagelok fittings. To prepare for a diffraction experiment, a sealing plug was removed and the tube quickly attached to the apparatus. Evacuation of the tube was immediate. The ReF_6 , OsF_6 , IrF_6 , and pure PtF_6 , samples were sent to Oregon State University in their reaction vessels equipped with Whitey valves. Once attached to the apparatus each of the sample containers was initially cooled down and evacuated to remove any excess F_2 . The WF_6 sample contained a small amount of SiF_4 which was removed by repeatedly cooling to approximately –78 °C, evacuating, and rewarming.

Most samples were introduced into the diffraction apparatus by immersing the sample containers in a bath at a temperature that produced convenient sample vapor pressures and then opening the valve to allow the gas to flow through the nozzle assembly and intersect the electron beam. The flow was continuous throughout the experiments. All MF_6 bulk samples required cooling to –45 °C to obtain suitable vapor pressures; the nozzle temperatures (i.e., the temperatures of the gases) were 23 °C. The O_2PtF_6 vapor phase was obtained by wrapping the bulk sample tubes with heating tape and heating to about 120 °C. For this sample the nozzle assembly was kept at 142–145 °C to avoid any possible condensation. Data for the diffraction experiments were as follows: sector, r^3 ; typical beam currents, 0.52–0.62 μA ; exposure times, 1.7–4.0 min; ambient apparatus pressure during run-in of sample, $(4.0\text{--}9.4) \times 10^{-6}$ Torr; photographic plates, 8 × 10 in Kodak projector slide (or electron image); development, 10 min in D-19 diluted 1:1; electron accelerating voltage, 60 kV; electron wavelength calibration, CO_2 ($r_a(\text{C}=\text{O}) = 1.1646 \text{ \AA}$, $r_a(\text{O}\cdots\text{O}) = 2.3244 \text{ \AA}$). Data for the O_2PtF_6 experiments were similar with the exceptions of elevated sample temperature and wavelength calibration against CS_2 ($r_a(\text{C}=\text{S}) = 1.557 \text{ \AA}$, $r_a(\text{S}\cdots\text{S}) = 3.109 \text{ \AA}$). In most cases three plates at each camera distance (75 and 30 cm) were chosen for analysis. The diffraction data are available in the Supporting Information.

(7) Bartlett, N. *Angew. Chem.* **1968**, *7*, 433.

(8) Bartlett, N.; Lohmann, D. H. *Proc. Chem. Soc.* **1962**, 115.

(9) Miller, B. R.; Bartlett, L. S. *J. Chem. Phys.* **1980**, *72*, 800.

(10) Almenningsen, A.; Bastiansen, O.; Trætteberg, M. *Acta Chem. Scand.* **1959**, *13*, 1699.

(11) Edwards, A. J.; Falconer, W. E.; Griffiths, J. E.; Sunder, W. A.; Vasile, M. J. *J. Chem. Soc., Dalton Trans.* **1974**, 1129.

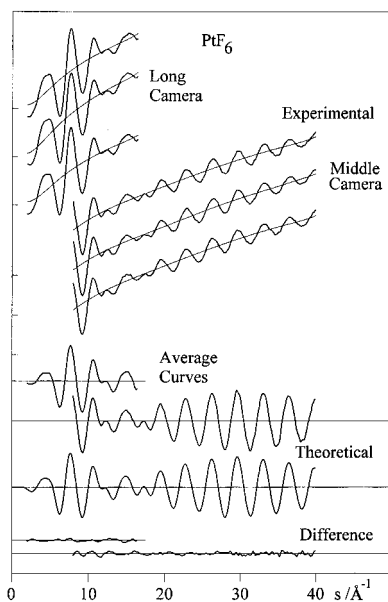


Figure 1. Intensity curves for PtF_6 . Curves of the data from each exposure are shown superimposed on their backgrounds. The average curves are the molecular intensities on which the refinements were based. The difference curves are experimental minus theoretical for the final model that includes allowance for multiple scattering.

Structure Analysis

Intensity Curves and Radial Distribution Curves. The experimental molecular intensity distributions ($sI_M(s)$) were obtained in a manner previously described.¹² Curves of the total intensity for each plate and averages of the molecular intensities from each camera distance are shown for PtF_6 in Figure 1. Figures of these curves for the other molecules and for O_2PtF_6 are obviously similar and are available as Supporting Information. The experimental radial distribution curves, $P(r)/r$, for all systems are shown in Figure 2. Each was calculated from a composite of the two average $sI_M(s)$ curves by adding theoretical intensity data from the final model for the unobserved region $0 \leq s/\text{Å}^{-1} \leq 2.5$ and multiplying the result by $Z_F^2/(A_F)^2 \exp(-0.002s^2)$. The distances corresponding to the three largest peaks of the radial distribution curves are obvious. In the case of the O_2PtF_6 sample there is also a small peak at 1.2 Å that corresponds to the bond length in an O_2 molecule.

Molecular Orbital Calculations. Ab initio optimizations of the structures of the five molecules were carried out with the program Gaussian 98W¹³ at several levels of theory with a variety of basis sets. The main object was to discover whether conditions could be found that would represent satisfactorily both the bond lengths and the bond-length trend observed

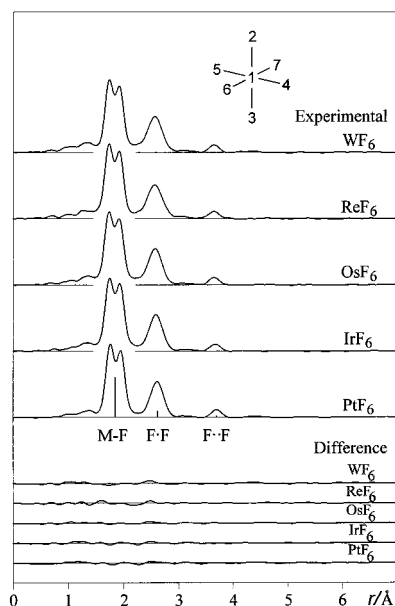


Figure 2. Radial distribution curves for third group transition-metal hexafluorides. The vertical bars show the positions and weights of the interatomic distances. The doubled peak corresponding to the M–F distance arises from phase-shift effects. The difference curves are experimental minus theoretical for the final models.

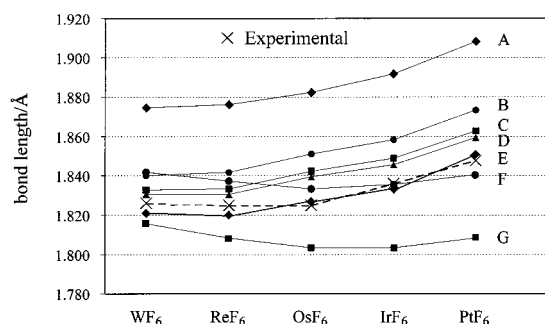


Figure 3. Experimental and theoretical bond lengths: (A) B3LYP/Stuttgart RSC (M), 6-311G* (F); (B) B3LYP/Hay-Wadt($n+1$)VDZ (M), aug-cc-pVTZ (F); (C) B3PW91/Hay-Wadt($n+1$)VDZ (M), aug-cc-pVTZ (F); (D) B3P86/Hay-Wadt($n+1$)VDZ (M), aug-cc-pVTZ (F); (E) MP2/Hay-Wadt($n+1$)VDZ (M), aug-cc-pVTZ (F); (F) HF/Stuttgart RSC (M), 6-311G* (F); (G) HF/Stuttgart RSC (M), aug-cc-pVTZ (F).

experimentally. O_h symmetry was assumed; however, as discussed below it is possible that a Jahn–Teller (J–T) effect¹⁴ exists in the cases of ReF_6 , OsF_6 , and IrF_6 ,¹⁹ and accordingly D_{4h} models were also optimized. Theoretical results for many of these calculations are found in Table 2, and plots of the bond-length trends are given in Figure 3.

Normal Coordinate Calculations. The effects of vibrational averaging in molecules are manifested by distances, each of which, when fitted by least squares without regard for the restrictions of an equilibrium symmetry, are not consistent with that symmetry. This distance type, r_a , may be converted to the geometrically consistent r_α type with use of corrections obtained from normal-coordinate calculations. The vibrational force fields on which the corrections depend were evaluated for each molecule in terms of the O_h symmetry coordinates defined by Pistorius¹⁵ (Table 3) fitted to the observed wavenumbers as summarized by Weinstock and Goodman (Table 4).¹⁶ Four of

- (12) (a) Data reduction: Gundersen, G.; Hedberg, K. *J. Chem. Phys.* **1969**, *51*, 2500. (b) Background removal: Hedberg, L. *Abstracts*, Fifth Austin Symposium on Gas-Phase Molecular Structure, Austin, TX, 1974; p 37.
- (13) Frisch, M. J.; Trucks, G. W.; Schlegel, H. B.; Scuseria, G. E.; Robb, M. A.; Cheeseman, J. R.; Zakrzewski, V. G.; Montgomery, J. A., Jr.; Stratmann, R. E.; Burant, J. C.; Dapprich, S.; Millam, J. M.; Daniels, A. D.; Kudin, K. N.; Strain, M. C.; Farkas, O.; Tomasi, J.; Barone, V.; Cossi, M.; Cammi, R.; Mennucci, B.; Pomelli, C.; Adamo, C.; Clifford, S.; Ochterski, J.; Petersson, G. A.; Ayala, P. Y.; Cui, Q.; Morokuma, K.; Malick, D. K.; Rabuck, A. D.; Raghavachari, K.; Foresman, J. B.; Cioslowski, J.; Ortiz, J. V.; Baboul, A. G.; Stefanov, B. B.; Liu, G.; Liashenko, A.; Piskorz, P.; Komaromi, I.; Gomperts, R.; Martin, R. L.; Fox, D. J.; Keith, T.; Al-Laham, M. A.; Peng, C. Y.; Nanayakkara, A.; Gonzalez, C.; Challacombe, M.; Gill, P. M. W.; Johnson, B.; Chen, W.; Wong, M. W.; Andres, J. L.; Gonzalez, C.; Head-Gordon, M.; Replogle, E. S.; Pople, J. A. *Gaussian 98*, Revision A.7, Gaussian, Inc.: Pittsburgh, PA, 1998.

(14) Jahn, H. A.; Teller, E. *Proc. R. Soc. London* **1937**, *A161*, 220.

(15) Pistorius, C. W. F. T. *J. Chem. Phys.* **1958**, *29*, 1328.

(16) Weinstock, B.; Goodman, G. L. In *Advances in Chemical Physics*; Progogine, I., Ed.; Interscience: New York, 1965; Vol IX, p 169.

Table 2. Ab Initio Results for PtF₆, IrF₆, OsF₆, ReF₆, and WF₆

molecule, symmetry	method	metal basis ^{a,b}	F basis ^a	E_h	$r_e^c/\text{\AA}$	$\Delta r^d/\text{\AA}$
WF ₆ , O_h	HF	Stgt. RSC	6-311G*	-663.299 3939	1.842 (F)	-0.016
	HF	Stgt. RSC	aug-cc-pVTZ	-663.475 1009	1.815 (G)	0.011
	B3LYP	Stgt. RSC	6-311G*	-666.578 4696	1.874 (A)	-0.048
	B3LYP	HW(<i>n</i> +1)VDZ	aug-cc-pVTZ	-667.406 0635	1.840 (B)	-0.014
	B3P86	HW(<i>n</i> +1)VDZ	aug-cc-pVTZ	-668.647 7481	1.830 (D)	-0.004
	B3PW91	HW(<i>n</i> +1)VDZ	aug-cc-pVTZ	-667.206 8863	1.833 (C)	-0.007
	MP2	HW(<i>n</i> +1)VDZ	aug-cc-pVTZ	-666.186 2820	1.821 (E)	0.005
	ReF ₆ , O_h	HF	Stgt. RSC	6-311G*	-674.260 2220	1.837 (F)
HF	Stgt. RSC	aug-cc-pVTZ	-674.438 9018	1.808 (G)	0.017	
B3LYP	Stgt. RSC	6-311G*	-677.637 2379	1.876 (A)	-0.051	
B3LYP	HW(<i>n</i> +1)VDZ	aug-cc-pVTZ	-678.533 3301	1.841 (B)	-0.016	
B3P86	HW(<i>n</i> +1)VDZ	aug-cc-pVTZ	-679.801 5094	1.831 (D)	-0.006	
B3PW91	HW(<i>n</i> +1)VDZ	aug-cc-pVTZ	-667.339 1072	1.833 (C)	-0.008	
MP2	HW(<i>n</i> +1)VDZ	aug-cc-pVTZ	-677.233 2744	1.820 (E)	0.005	
D_{4h}	B3P86	HW(<i>n</i> +1)VDZ	aug-cc-pVTZ	-679.802 7495	{ 1.804 ^e 1.844 ^f	{ 0.021 -0.019
OsF ₆ , O_h	HF	Stgt. RSC	6-311G*	-686.399 0396	1.833 (F)	-0.008
	HF	Stgt. RSC	aug-cc-pVTZ	-686.567 7347	1.804 (G)	0.021
	B3LYP	Stgt. RSC	6-311G*	-689.887 5997	1.882 (A)	-0.057
	B3LYP	HW(<i>n</i> +1)VDZ	aug-cc-pVTZ	-690.351 1245	1.851 (B)	-0.026
	B3P86	HW(<i>n</i> +1)VDZ	aug-cc-pVTZ	-691.644 9295	1.839 (D)	-0.014
	B3PW91	HW(<i>n</i> +1)VDZ	aug-cc-pVTZ	-690.161 0208	1.842 (C)	-0.017
	MP2	HW(<i>n</i> +1)VDZ	aug-cc-pVTZ	-688.991 8332	1.827 (E)	-0.002
	D_{4h}	B3P86	HW(<i>n</i> +1)VDZ	aug-cc-pVTZ	-691.649 0621	{ 1.790 ^e 1.864 ^f
IrF ₆ , O_h	HF	Stgt. RSC	6-311G*	-699.899 6950	1.836 (F)	0.000
	HF	Stgt. RSC	aug-cc-pVTZ	-700.060 4027	1.804 (G)	0.032
	B3LYP	Stgt. RSC	6-311G*	-703.467 8215	1.892 (A)	-0.056
	B3LYP	HW(<i>n</i> +1)VDZ	aug-cc-pVTZ	-703.903 2953	1.859 (B)	-0.023
	B3P86	HW(<i>n</i> +1)VDZ	aug-cc-pVTZ	-705.222 0217	1.846 (D)	-0.010
	B3PW91	HW(<i>n</i> +1)VDZ	aug-cc-pVTZ	-703.716 6633	1.849 (C)	-0.013
	MP2	HW(<i>n</i> +1)VDZ	aug-cc-pVTZ	-702.463 1908	1.833 (E)	0.003
	D_{4h}	B3P86	HW(<i>n</i> +1)VDZ	aug-cc-pVTZ	-705.224 2922	{ 1.881 ^e 1.828 ^f
PtF ₆ , O_h	HF	Stgt. RSC	6-311G*	-714.689 2499	1.841 (F)	0.007
	HF	Stgt. RSC	aug-cc-pVTZ	-714.842 5337	1.808 (G)	0.040
	B3LYP	Stgt. RSC	6-311G*	-718.337 8680	1.908 (A)	-0.060
	B3LYP	HW(<i>n</i> +1)VDZ	aug-cc-pVTZ	-718.218 8543	1.873 (B)	-0.025
	B3P86	HW(<i>n</i> +1)VDZ	aug-cc-pVTZ	-719.561 4430	1.860 (D)	-0.012
	B3PW91	HW(<i>n</i> +1)VDZ	aug-cc-pVTZ	-718.034 3265	1.863 (C)	-0.015
	MP2	HW(<i>n</i> +1)VDZ	aug-cc-pVTZ	-716.711 3127	1.850 (E)	0.002

^a Basis sets from the Extensible Computational Chemistry Environment Basis Set Database, Version 1.0, as developed and distributed by the Molecular Science Computing Facility, Environmental and Molecular Sciences Laboratory which is part of the Pacific Northwest Laboratory, P.O. Box 999, Richland, WA 99352, and funded by the U.S. Department of Energy. The Pacific Northwest Laboratory is a multiprogram laboratory operated by Battelle Memorial Institute for the U.S. Department of Energy under Contract DE-AC06-76RLO 1830. Contact David Feller or Karen Schuchardt for further information. ^b Stgt. RSC, Stuttgart relativistic small core effective core potential; HW(*n*+1)VDZ, Hay-Wadt (*n*+1) VDZ effective core potential. See footnote *a* for references to original articles. ^c Letters identify corresponding curves of Figure 3. ^d Experimental minus theoretical bond-length values. ^e Axial bond. ^f Equatorial bond.

Table 3. Symmetry Coordinates for MF₆ Molecules^a

mode	coordinates ^b
a_{1g}	$S_1 \quad 1/\sqrt{6}\Delta(r_2 + r_3 + r_4 + r_5 + r_6 + r_7)$
e_g	$S_{2a} \quad 1/\sqrt{8}\Delta(2r_2 + 2r_3 - r_4 - r_5 - r_6 - r_7)$
	$S_{2b} \quad 1/2\Delta(r_6 + r_7 - r_4 - r_5)$
f_{1u}	$S_{3x} \quad 1/\sqrt{2}\Delta(r_2 - r_3)$
	$S_{3y} \quad 1/\sqrt{2}\Delta(r_6 - r_7)$
	$S_{3z} \quad 1/\sqrt{2}\Delta(r_4 - r_5)$
f_{1u}	$S_{4x} \quad 1/\sqrt{8}\Delta(\alpha_{34} + \alpha_{35} + \alpha_{36} + \alpha_{37} - \alpha_{24} - \alpha_{25} - \alpha_{26} - \alpha_{27})$
	$S_{4y} \quad 1/\sqrt{8}\Delta(\alpha_{27} + \alpha_{37} + \alpha_{47} + \alpha_{57} - \alpha_{26} - \alpha_{36} - \alpha_{46} - \alpha_{56})$
	$S_{4z} \quad 1/\sqrt{8}\Delta(\alpha_{25} + \alpha_{35} + \alpha_{56} + \alpha_{57} - \alpha_{24} - \alpha_{34} - \alpha_{46} - \alpha_{47})$
f_{2g}	$S_{5x} \quad 1/2\Delta(\alpha_{47} + \alpha_{56} - \alpha_{46} - \alpha_{57})$
	$S_{5y} \quad 1/2\Delta(\alpha_{27} + \alpha_{36} - \alpha_{26} - \alpha_{37})$
	$S_{5z} \quad 1/2\Delta(\alpha_{25} + \alpha_{34} - \alpha_{24} - \alpha_{35})$
f_{2u}	$S_{6x} \quad 1/\sqrt{8}\Delta(\alpha_{24} + \alpha_{25} + \alpha_{36} + \alpha_{37} - \alpha_{34} - \alpha_{35} - \alpha_{26} - \alpha_{27})$
	$S_{6y} \quad 1/\sqrt{8}\Delta(\alpha_{46} + \alpha_{56} + \alpha_{27} + \alpha_{37} - \alpha_{47} - \alpha_{57} - \alpha_{26} - \alpha_{36})$
	$S_{6z} \quad 1/\sqrt{8}\Delta(\alpha_{46} + \alpha_{47} + \alpha_{25} + \alpha_{36} - \alpha_{24} - \alpha_{34} - \alpha_{56} - \alpha_{57})$

^a From ref 15. ^b Subscripts indicate bonds or angles between bonds. See Figure 2.

the six normal modes are found alone in symmetry species a_{1g} , e_g , t_{2g} , and t_{2u} , and thus the force constants are uniquely

determined. The remaining two of symmetry t_{1u} give rise to three force constants, one of which requires an arbitrary choice within a range of acceptable values. The choice was made with use of the program ASYM40¹⁷ by symmetrization of the theoretical Cartesian force constants calculated at the B3P86/(HW(*n*+1)VDZ (M); aug-cc-pVTZ (F)) level (see footnote *b* Table 2) followed by adjustment of scale constants applied to these preliminary symmetrized force constants to fit the observed wavenumbers. The force fields that resulted from this procedure are shown in Table 4, where one notes that the values of the bond-stretch force constants drop off for the iridium and platinum compounds in accordance with the well-known inverse relationship between force constants and bond lengths. The distance corrections ($r_a - r_\alpha$) may be deduced from Table 5.

Results of Structure Refinements. Refinements of each structure were done as usual by a simultaneous least-squares fitting of theoretical intensity data to the two sets of average experimental intensities.¹⁸ Since we wished to take account of the effects of multiple scattering, and since the refinement

(17) Hedberg, L.; Mills, I. M. *J. Mol. Spectrosc.* **1993**, *160*, 117.

(18) Hedberg, K.; Iwasaki, M. *Acta Crystallogr.* **1964**, *17*, 529.

Table 4. Force Constants and Wavenumbers for Third Row Transition-Metal Hexafluorides

	force constants/($\text{md}\cdot\text{\AA}^{-1}$)					wavenumbers ^a / cm^{-1}					
	WF ₆	ReF ₆	OsF ₆	IrF ₆	PtF ₆	WF ₆	ReF ₆	OsF ₆	IrF ₆	PtF ₆	
symmetry											
F_{11}	6.65	6.38	6.01	5.50	4.80	ν_1	771	755	733	701	655
F_{22}	5.07	5.04	4.99	4.67	4.03	ν_2	673	671	668	646	600
F_{33}	4.73	4.80	4.88	4.88	4.70	ν_3	711	715	720	719	705
F_{34}	-0.21	-0.21	-0.23	-0.23	-0.23						
F_{44}	0.93	0.93	1.05	1.09	1.09	ν_4	258	257	272	276	273
F_{55}	0.93	0.82	0.72	0.63	0.57	ν_5	315	295	276	258	242
F_{66}	0.34	0.70	0.80	0.81	0.86	ν_6	134	193	205	206	211
internal bond-stretching											
$f_{\text{M-F}}$	5.17	5.14	5.11	4.91	4.49						

^a Reference 16.**Table 5.** Distances ($r/\text{\AA}$) and Amplitudes of Vibration ($l/\text{\AA}$) in PtF₆, IrF₆, OsF₆, ReF₆, and WF₆^a

	multiple scattering included					multiple scattering excluded				
	r_{α}	r_{g}	r_{a}	l	R^b	r_{α}	r_{g}	r_{a}	l	R
Octahedral Symmetry Assumed										
WF ₆										
W-F	1.824	1.829(2)	1.828	0.043(2)	0.094	1.825	1.830(2)	1.829	0.041(2)	0.152
F-F	2.580	2.587(3)	2.583	0.098(7)		2.581	2.588(3)	2.584	0.095(10)	
F··F	3.649	3.650(4)	3.649	0.058(14)		3.651	3.652(4)	3.651	0.056(22)	
ReF ₆										
Re-F	1.825	1.829(2)	1.828	0.043(2)	0.125	1.826	1.830(2)	1.829	0.041(3)	0.178
F-F	2.581	2.586(3)	2.581	0.105(9)		2.582	2.587(3)	2.583	0.101(12)	
F··F	3.650	3.652(4)	3.651	0.056(19)		3.652	3.654(5)	3.653	0.052(25)	
OsF ₆										
Os-F	1.825	1.828(2)	1.827	0.048(2)	0.091	1.826	1.829(2)	1.828	0.046(2)	0.159
F-F	2.580	2.584(3)	2.581	0.094(6)		2.582	2.586(3)	2.582	0.090(9)	
F··F	3.649	3.651(4)	3.650	0.064(14)		3.651	3.653(4)	3.652	0.061(24)	
IrF ₆										
Ir-F	1.836	1.839(2)	1.838	0.047(2)	0.099	1.837	1.840(2)	1.839	0.046(2)	0.153
F-F	2.596	2.600(3)	2.597	0.090(6)		2.597	2.601(3)	2.598	0.088(8)	
F··F	3.671	3.673(4)	3.672	0.065(17)		3.673	3.675(5)	3.674	0.062(24)	
PtF ₆										
Pt-F	1.848	1.852(2)	1.851	0.046(2)	0.081	1.850	1.853(2)	1.852	0.045(2)	0.151
F-F	2.614	2.618(3)	2.615	0.091(6)		2.616	2.619(3)	2.618	0.088(8)	
F··F	3.697	3.699(4)	3.698	0.061(13)		3.699	3.702(5)	3.701	0.060(24)	
PtF ₆ (from O ₂ PtF ₆)										
Pt-F	1.846	1.851(2)	1.850	0.044(2)	0.121	1.847	1.852(2)	1.851	0.044(2)	0.157
F-F	2.611	2.616(3)	2.612	0.100(9)		2.613	2.618(3)	2.614	0.098(10)	
F··F	3.692	3.695(4)	3.694	0.062(21)		3.695	3.698(5)	3.697	0.061(26)	
O-O		1.205	1.205(18)	0.030(33)			1.213	1.213(23)	0.027(45)	
X(O ₂)		0.42					0.41			
Three Independent Distances										
WF ₆										
W-F		1.829(2)	1.828	0.043(2)	0.089		1.830(2)	1.829	0.041(2)	0.149
F-F		2.576(7)	2.572	0.097(7)			2.575(11)	2.571	0.093(9)	
F··F		3.650(17)	3.649	0.057(14)			3.649(26)	3.648	0.055(22)	
ReF ₆										
Re-F		1.829(2)	1.828	0.043(2)	0.120		1.830(2)	1.829	0.041(3)	0.174
F-F		2.572(10)	2.567	0.103(9)			2.571(14)	2.567	0.099(12)	
F··F		3.651(22)	3.650	0.055(18)			3.651(28)	3.650	0.051(24)	
OsF ₆										
Os-F		1.828(2)	1.827	0.048(2)	0.089		1.829(2)	1.828	0.046(2)	0.159
F-F		2.579(6)	2.576	0.094(6)			2.578(10)	2.575	0.090(9)	
F··F		3.651(17)	3.650	0.064(14)			3.651(29)	3.650	0.060(24)	
IrF ₆										
Ir-F		1.839(2)	1.838	0.047(2)	0.103		1.840(2)	1.839	0.046(2)	0.158
F-F		2.593(7)	2.590	0.090(6)			2.592(10)	2.589	0.087(9)	
F··F		3.676(22)	3.675	0.065(18)			3.676(31)	3.674	0.062(26)	
PtF ₆										
Pt-F		1.852(2)	1.851	0.046(2)	0.080		1.853(2)	1.852	0.045(2)	0.149
F-F		2.613(6)	2.610	0.090(6)			2.612(9)	2.609	0.088(8)	
F··F		3.697(16)	3.696	0.061(13)			3.696(28)	3.695	0.059(23)	

^a Values in parentheses are 2σ and include estimates of data correlation and systematic error. ^b Goodness of fit factor: $R = [\sum_i w_i \Delta_i^2 / \sum_i I_i (\text{obsd})^2]^{1/2}$, where $\Delta_i = I_i(\text{obsd}) - I_i(\text{calcd})$ with $I_i = s_i I_i$.

program does not allow for changes in the multiple-scattering contribution during cycling, the procedure for inclusion of these effects was to calculate their contribution for a trial model and

add them to the theoretical two-atom scattering being fitted. The three-atom scattering contribution was upgraded as the cycling proceeded so that in the end it corresponded to the final

model. With assumption of O_h symmetry for each molecule, the convenient parameters are the M–F bond length and the three vibrational amplitudes corresponding to the M–F, F···F (90°), and F···F (180°) distances. The distances were defined in r_a space. However, since the three distances are well-resolved, they may also be refined independently in r_a space. This was done in each case (except for the refinements on the data from the O_2PtF_6 sample) in anticipation of obtaining an estimate of vibrational averaging effects through comparison of corresponding distances from these two types of models. Since (see below) the molecule most likely to display the result of Jahn–Teller distortion is OsF_6 , models of it having two different bond lengths and D_{4h} symmetry were also tested.

As expected, the refinements of all models of O_h symmetry and all consisting of three independent distances converged quickly. The results are summarized in Table 5. The correlation matrices are omitted because the parameters are either 100% correlated (nonbond distances with bond distances in models of O_h symmetry) or essentially uncorrelated (all distances with vibrational amplitudes in both model types as well as distances with each other in the models unconstrained by symmetry). Visual evidence of the quality of the fits is seen in the difference curves of Figures 1 and 2 and in the figures of the Supporting Information. The attempted refinements of OsF_6 structures with D_{4h} symmetry (either axial or equatorial bonds the longer) did not converge, but tended to revert to structures of O_h symmetry.

Discussion

Our gas-phase structure determinations of the five-third row transition-metal hexafluorides leave no doubt that the bonds in IrF_6 and in the previously unmeasured PtF_6 are longer than those in the tungsten, rhenium, and osmium compounds. The results agree with the early GED work for the tungsten, rhenium, and osmium compounds,^{2–4} and although the Ir–F bond is found to be longer than previously measured,³ it lies within the uncertainty quoted in that investigation. Our results for IrF_6 (and for PtF_6) have small bond-length uncertainties comparable to the other molecules and thus reveal the distance trend more precisely. The fact that our distance values do not disagree with the older ones (all measurements fall within the ranges defined by the uncertainties), but disprove the assumption of bond-length equality, points to the importance of heeding the uncertainties when drawing conclusions about distance differences.

It has been proposed¹⁹ that since ReF_6 , OsF_6 , and possibly IrF_6 have orbitally degenerate electronic ground states, their nominally octahedral symmetry should be lowered by the Jahn–Teller effect.¹⁴ Support for this idea is provided by an analysis of the spectra of the rhenium and osmium compounds,¹⁹ some aspects of which are abnormal compared to the spectra of WF_6 and PtF_6 which are not expected to exhibit J–T distortion. (Curiously, IrF_6 , which is also a candidate for J–T distortion, apparently does not show these spectral abnormalities.) Operation of the J–T effect in OsF_6 is also suggested by its structure in the crystal,⁶ where the molecules were found have an average axial bond length about 0.02 \AA greater than the equatorial average—a distortion judged to be in excess of that expected from crystal packing forces. We have sought evidence of the J–T effect through molecular orbital calculations (Table 2). The results for ReF_6 , OsF_6 , and IrF_6 show that models of D_{4h} symmetry are slightly more stable than those of O_h symmetry for the level of theory and basis sets tested. The reliability of

these calculations is uncertain since a similar test with PtF_6 where no distortion is expected gave a similar result. In any case it was verified by tests of some D_{4h} models that, based on the quality of agreement, our electron-diffraction data are indeed capable of detecting bond-length differences greater than about 0.05 \AA . Thus, our work ensures that if distortions from O_h symmetry exist in any of these molecules, they must give rise to bond lengths differing by no more than this amount.

Table 5 offers comparisons of the structural results from the experiments on O_2PtF_6 and PtF_6 as well as of the effects of multiple (three-atom) scattering on all the molecules. It is seen that apart from the presence of molecular oxygen in the diffraction patterns from O_2PtF_6 , the structures derived from it and from pure PtF_6 are essentially identical. (The mole fraction of O_2 in the O_2PtF_6 results is less than the theoretical 0.5 because the lower mass of the former causes more of it to diffuse at higher angles from the nozzle tip and thus to avoid entering the scattering region.) Allowance for the effect of multiple scattering significantly improves the quality of agreement in all cases, as the agreement factor R shows, although the values of the parameters, interatomic distances, and vibrational amplitudes are scarcely affected.

The effects of vibrational averaging, or “shrinkage”, in our hexafluorides manifest themselves in the values of the nonbond interatomic distances for the independent distance models. These distances are in each case shorter than expected on the basis of the bond-length measurements and the assumption of O_h symmetry for the molecules; i.e., $r_g(F\cdot F) = \sqrt{2}r_g(M-F)$ and $r_g(F\cdot F) = 2r_g(M-F)$. For the models with multiple scattering included the shortenings average about 0.009 \AA for $r_g(F\cdot F)$ and 0.005 \AA for $r_g(F\cdot F)$. The values are similar for r_a shrinkages and slightly larger for the models without multiple scattering. These are experimental shrinkages. The corresponding average “theoretical” shrinkages (the difference between a nonbond distance and that predicted from the bond length assuming O_h symmetry) are 0.001 and 0.005 \AA . Although the latter is in excellent agreement with experiment, the former is not. The reason is unclear, but vibrational anharmonicity, which was not taken into account in these models, may play a role.

The bond lengths from the ab initio calculations (Table 2 and Figure 3) vary over a wide range. To assess the level of theory and basis set combinations that give the best fit to experiment, we look for both the agreement between theoretical and experimental distance values and evidence of the upward trend in these values toward the end of the series. As Figure 3 shows, models calculated at the B3LYP level with the Stgt RSC metal basis and the 6-311G* basis for fluorine (curve A) exhibit the observed trend across the series, but bond lengths are much too large. Results at the HF level with the Stgt RSC metal basis and the aug-cc-pVTZ fluorine basis (curve G) include distance values in better agreement on average, but this time too small; moreover the distance trend across the series is the opposite of that observed experimentally. Good agreement with the experimental bond lengths is found from the HF/(Stgt.RSC (M); 6-311G* (F)) calculations (curve F), but here again the distance trend is not seen. Better agreement is given by the calculations at the B3P86/(HW($n+1$))VDZ (M); aug-cc-pVTZ (F)) level (curve D) and by those at the B3PW91 level with the same bases (curve C); in both cases the distance trend is well-reproduced and the average distance difference ($r_a(\text{obs}) - r_a(\text{calc})$) is only -0.009 to -0.011 \AA . Results at the B3LYP level with these bases show the desired trend with slightly poorer agreement with the observed distances (curve B). The best fit to experiment is provided by the MP2/(HW($n+1$))VDZ (M); aug-

(19) Weinstock, B.; Claassen, H. H.; Malm, J. G. *J. Chem. Phys.* **1960**, *32*, 181.

cc-pVTZ (F)) calculations, where both the distance values and trend are very well-reproduced—here the difference $r_{\alpha}(\text{obs}) - r_{\alpha}(\text{calc})$ averages only -0.0026 \AA with the theoretical values the smaller as they should be. Not shown in the table are several additional calculations that were carried out in the case of OsF_6 in order to establish the effect of other combinations of basis set and level of theory, but none of these gave an appreciably better fit to the observed distance than the best of those cited above. On the basis of the data of Table 2 as rendered in Figure 3, we conclude that for the third row transition-metal hexafluorides (1) Hartree–Fock theory does not reproduce the distance trend observed for the series, although a relativistic, small-core (RSC) basis set for the metals combined with a 6-311G* basis for fluorine reproduces the distance values quite well; (2) density functional theory reproduces the trend very nicely, but the RSC and 6-311G* bases give poor agreement with the distances themselves; and (3) density functional- or MP2-level theory with the Hay–Wadt effective core potential basis for the metals combined with the augmented correlation consistent basis for fluorine is necessary for reproducing satisfactorily both the trend and the distance values.

In the following paper in this issue, Graudejus et al. offer an appealing picture of the distance trends in the second and third row transition-metal hexafluorides, both as neutral species and as singly charged anions. So far as our neutral MF_6 molecules are concerned, the important matters are the following; the paper cited should be consulted for more details. As the nuclear charge increases across the series, the electrons added in each step occupy a dt_{2g} orbital largely centered on the metal atom and operate to partially shield the nuclear charge. The result of this

shielding is that the bond length in the tungsten, rhenium, and osmium compounds remains essentially unchanged as the nuclear charge increases. Why does this phenomenon not extend to IrF_6 and PtF_6 ? It has been noted that, in contrast to the first three members of the series, both IrF_6 and PtF_6 are powerful oxidizing agents,^{7,8} PtF_6 more potent than IrF_6 , both capable of generating elemental fluorine from fluoride ion. This suggests that the energies of the dt_{2g} orbitals of these two compounds are close to the nonbonding fluorine orbitals which facilitates transfer of charge to the metals, a transfer likely to be easier for PtF_6 . The result is an increased shielding of the metal charges, greater in the case of PtF_6 , and a corresponding lengthening of the bonds which is accordingly also greater for PtF_6 .

Acknowledgment. This work was supported by the National Science Foundation under Grant CHE95-23581 to Oregon State University and by the Director, Office of Energy Research, Office of Basic Energy Sciences, Chemical Science and Materials Science Divisions of the U. S. Department of Energy under Contract No. DE-AC-03-76SF00098 with the University of California, Berkeley. We are grateful to Professor Neil Bartlett for suggesting the PtF_6 project and for many helpful comments during the course of the work. We thank Professor Gary Gard for the sample of WF_6 .

Supporting Information Available: Tables of the scattered intensity from all MF_6 molecules and from the sample of O_2PtF_6 and figures of the intensity curves from all experiments. This material is available free of charge via the Internet at <http://pubs.acs.org>.

IC000003C